





Article

Effects of Silica Nanoparticles on the Piezoelectro-Elastic Response of PZT-7A–Polyimide Nanocomposites: Micromechanics Modeling Technique

Usama Umer ^{1,*}, Mustufa Haider Abidi ¹, Syed Hammad Mian ¹, Fahad Alasim ^{1,2}
and Mohammed K. Aboudaif ¹

¹ Advanced Manufacturing Institute, King Saud University, P.O. Box 800, Riyadh 11421, Saudi Arabia

² Industrial Engineering Department, College of Engineering, King Saud University, P.O. Box 800, Riyadh 11421, Saudi Arabia

* Correspondence: uumer@ksu.edu.sa

Abstract: By using piezoelectric materials, it is possible to convert clean and renewable energy sources into electrical energy. In this paper, the effect on the piezoelectro-elastic response of piezoelectric-fiber-reinforced nanocomposites by adding silica nanoparticles into the polyimide matrix is investigated by a micromechanical method. First, the Ji and Mori–Tanaka models are used to calculate the properties of the nanoscale silica-filled polymer. The nanoparticle agglomeration and silica–polymer interphase are considered in the micromechanical modeling. Then, considering the filled polymer as the matrix and the piezoelectric fiber as the reinforcement, the Mori–Tanaka model is used to estimate the elastic and piezoelectric constants of the piezoelectric fibrous nanocomposites. It was found that adding silica nanoparticles into the polymer improves the elastic and piezoelectric properties of the piezoelectric fibrous nanocomposites. When the fiber volume fraction is 60%, the nanocomposite with the 3% silica-filled polyimide exhibits 39%, 31.8%, and 37% improvements in the transverse Young’s modulus E_T , transverse shear modulus G_{TL} , and piezoelectric coefficient e_{31} in comparison with the composite without nanoparticles. Furthermore, the piezoelectro-elastic properties such as E_T , G_{TL} , and e_{31} can be improved as the nanoparticle diameter decreases. However, the elastic and piezoelectric constants of the piezoelectric fibrous nanocomposites decrease once the nanoparticles are agglomerated in the polymer matrix. A thick interphase with a high stiffness enhances the nanocomposite’s piezoelectro-elastic performance. Also, the influence of volume fractions of the silica nanoparticles and piezoelectric fibers on the nanocomposite properties is studied.

Keywords: PZT–polyimide composite; silica nanoparticle; piezoelectro-elastic properties; interphase; micromechanics modeling



Citation: Umer, U.; Abidi, M.H.; Mian, S.H.; Alasim, F.; Aboudaif, M.K. Effects of Silica Nanoparticles on the Piezoelectro-Elastic Response of PZT-7A–Polyimide Nanocomposites: Micromechanics Modeling Technique. *Polymers* **2024**, *16*, 2860. <https://doi.org/10.3390/polym16202860>

Academic Editor: Rafał Grzejda

Received: 15 September 2024

Revised: 4 October 2024

Accepted: 7 October 2024

Published: 10 October 2024



Copyright: © 2024 by the authors. Licensee MDPI, Basel, Switzerland. This article is an open access article distributed under the terms and conditions of the Creative Commons Attribution (CC BY) license (<https://creativecommons.org/licenses/by/4.0/>).

1. Introduction

Piezoelectric-fiber-reinforced polymer composites are used for various engineering applications, such as in clean energy harvester devices from environmental sources and in vibration control, structural health monitoring, and structural morphing [1–4]. The improved mechanical flexibility, good stiffness/strength-to-weight ratio, reliability, and tailorable properties have made piezoelectric fibrous composites more favorable for the abovementioned applications as compared to neat piezoelectric materials [4–8]. Nevertheless, advances in electro-mechanical technologies have led to fast growth in the demand for piezoelectric fibrous composites with better functionalities. So, the design of new piezoelectric composites is an important issue for researchers and scientists.

The concept of using nano/micro-hybrid reinforcements in polymer composites has emerged for the sake of improving their multifunctional properties. In these composites, nano-sized reinforcements such as graphene nanoplatelets, carbon nanotubes (CNTs), and silica nanoparticles are introduced alongside traditional micron-sized fibers [8–13]. For

example, Cui et al. [13] observed that carbon fiber–silica nanoparticle composites have better performance regarding interlaminar shear strength, impact strength, and flexural strength compared with that of carbon fiber composites. Hwayyin et al. [14] indicated an enhancement in the mechanical properties of carbon fiber–polyester composites at different weights of nano-silicon dioxide. The outcomes showed an increment in the tensile stress of 11.45% after an increase in the nanoparticle content from 0.16% wt. to 0.2% wt. [14]. Zheng et al. [15] studied the influence of silica nanoparticles on the mechanical properties of glass-fiber-reinforced epoxy composites. It was observed that the increase in the silica nanoparticle content yields an enhancement in the tensile modulus and compression strength. Gang et al. [16] reported that an increase from 0% to 5% of the nanoparticle volume fraction yielded an enhancement in the tensile modulus of a carbon fiber–silica nanoparticle–polyimide composite from 2475 MPa to 2780 MPa. Tang et al. [17] measured tensile properties in the transverse direction, interlaminar shear strength, and the mode I and mode II interlaminar fracture toughness of carbon fiber composites with 10 wt% and 20 wt% silica nanoparticles dispersed into epoxy. The transverse tensile properties and mode I interlaminar fracture toughness were improved by increasing the silica nanoparticle content in the epoxy [17].

Such a concept has been employed to study the advantages of nanofiller-containing matrices in improving the equivalent properties of piezoelectric fibrous composites. Keramati et al. [12] analyzed a nanocomposite in which BaTiO₃ fibers were placed inside a graphene nanosheet (GNS)-filled polymer. The addition of GNSs inside the polymer matrix led to an improvement in the elastic properties, transverse coefficient of thermal expansion, and piezoelectric coefficients e_{31} and e_{15} . The mechanical and piezoelectric characteristics of piezoelectric fiber–CNT-reinforced nanocomposites were investigated by Hasanzadeh et al. [18]. CNTs were randomly oriented into a polymer matrix. The mechanical properties and piezoelectric coefficient e_{31} of the piezoelectric nanocomposite containing CNTs were improved over those of the piezoelectric composite without CNTs [18]. Godara and Mahato [19] studied the elastic and piezoelectric coefficients of a nanocomposite in which piezoelectric fibers were embedded into a CNT-reinforced polymer [19]. The use of CNTs in piezoelectric-fiber-reinforced composites can enhance the structural/functional properties [19].

Generally, evaluating the engineering constants of piezoelectric fibrous nanocomposites containing silica nanoparticles is crucial in designing structures constructed with these materials. Many microstructural factors such as the amount, size, dispersion quality, variation in properties, and nanoparticle–matrix interfacial interaction affect the overall properties of silica-nanoparticle-containing composites [20–22]. Therefore, conducting studies in this area is of significance [9,18,23–26].

To the best of the authors' knowledge, the piezoelectro-elastic properties of piezoelectric fiber–nanoparticle–polymer nanocomposites with regard to the agglomeration and size of the silica nanoparticles and the silica–polymer interphase have not yet been sufficiently investigated. The novelty of this work comes from developing a hierarchical micromechanical method to comprehensively investigate the elastic and piezoelectric constants of PZT-7A–silica–polyimide nanocomposites with variables of important microstructures. So, the current research aims to evaluate the properties of a piezoelectric nanocomposite made of unidirectional piezoelectric fibers embedded in a polyimide matrix with silica nanoparticles. To achieve this, we developed a model using Ji's approach and the Mori–Tanaka method. After confirming the accuracy of the model, we studied how the volume, size, and clumping of nanoparticles, as well as the thickness and stiffness of the silica–polymer interface, affect the composite's elastic and shear moduli and piezoelectric coefficients (e_{31} and e_{33}). One potential use for these nanocomposites is in energy-harvesting devices.

2. Micromechanical Analysis of Piezoelectric Fibrous Nanocomposites

The nanocomposite consists of unidirectional piezoelectric microfibers, silica nanoparticles, and a polymer matrix. Figure 1 shows a representation of a lamina made of this

piezoelectric fibrous nanocomposite. The configuration of such a nanocomposite is such that piezoelectric fibers are embedded inside a nanoparticle-filled polymer. Note that the piezoelectric fibers are aligned along the 3-direction. The dispersion of the silica nanoparticles into the polymer matrix can be uniform or non-uniform. The interphase region shown in this figure is considered due to the interaction between the nanoparticles and the polymer matrix. In general, the representative volume element (RVE) of the nanocomposite system may be treated as consisting of two phases, in which the reinforcement is the piezoelectric fiber and the matrix is the nanoparticle-filled polymer. The micromechanical modeling to predict the effective properties of piezoelectric fibrous nanocomposites is carried out here in a two-step procedure. First, the elastic properties of the silica-nanoparticle-filled polymer are calculated using the Ji and Mori–Tanaka models. Next, the Mori–Tanaka model is employed to predict the overall piezoelectric coefficients and elastic moduli of the piezoelectric fibrous nanocomposite.

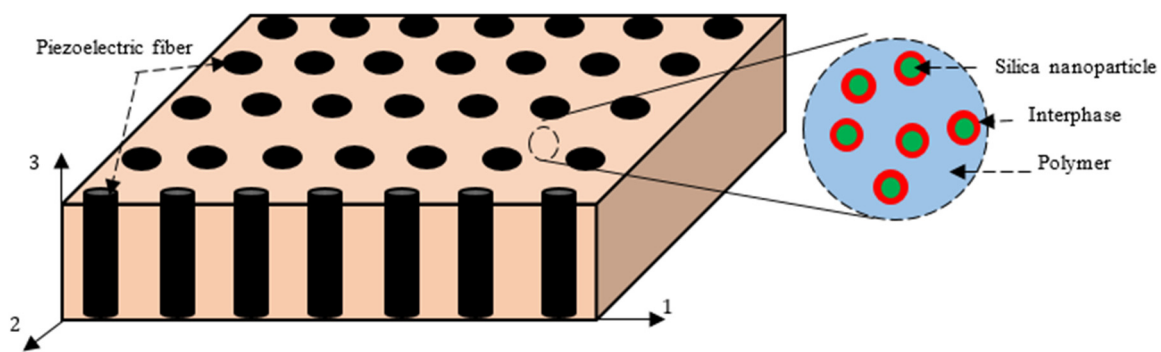


Figure 1. Demonstration of the piezoelectric fibrous nanocomposite with a silica-nanoparticle-filled polymer matrix.

2.1. Silica-Nanoparticle-Filled Polymer

In this sub-section, a micromechanics approach is presented to estimate the effective properties of the polymer matrix containing silica nanoparticles. Micromechanical models predict the composite properties in terms of the volume fraction, geometry of fillers, and material properties of constituents [27–30]. Concerning the nanoparticle-filled polymer systems, it is required to incorporate the interphase between the nanoparticle and the polymer matrix in the simulation [20,29,31–33]. The interfacial region possesses material properties in between those of the polymer matrix and those of the nanoparticle [20,22,31,32,34]. In the micromechanical simulation, the interphase is considered as the third phase, which surrounds the silica nanoparticles, as shown in Figure 1. The Young’s modulus of the silica-filled polymer materials with the interphase can be estimated by the Ji model [35,36] as follows:

$$E_{NC} = E_m \left[(1 - \lambda) + \frac{\lambda - \beta}{(1 - \lambda) + \frac{\lambda(k-1)}{\ln k}} + \frac{\beta}{(1 - \lambda) + \frac{(\lambda - \beta)(k+1)}{2} + \beta \frac{E_{NP}}{E_m}} \right]^{-1} \quad (1)$$

in which E_m and E_{NP} are the Young’s moduli of the matrix and nanoparticle, respectively. The values of λ , β , and k are given by

$$\lambda = \sqrt{\left(\frac{2t_i}{d_{NP}} + 1 \right)^3 \varphi_{NP}}, \quad \beta = \sqrt{\varphi_{NP}}, \quad k = \frac{E_i}{E_m} \quad (2)$$

where φ_{NP} and d_{NP} are the volume fraction and diameter of the nanoparticle, and E_i and t_i are the Young’s modulus and thickness of the interphase, respectively. The Young’s modulus of the silica-filled polymer materials in the absence of the interphase, i.e., a two-phase composite, is [36]

$$E_{NC} = E_m \left[(1 - \beta) + \frac{\beta}{(1 - \beta) + \beta \frac{E_{NP}}{E_m}} \right]^{-1} \tag{3}$$

Poisson’s ratio of a nanoparticle-filled polymer can be estimated by the rule of the mixture as $\nu_{NC} = \nu_{NP}\phi_{NP} + \nu_m(1 - \phi_{NP})$, in which ν_{NP} and ν_m are Poisson’s ratio of the nanoparticle and matrix, respectively.

Silica nanoparticles tend to form agglomerates, which leads to poor distribution into the polymer matrix during the fabrication process [20,37,38]. The non-uniform distribution and formation of nanoparticle agglomeration may be mostly attributed to their great specific surface area and high surface energy [37,38]. A two-parameter micromechanical technique is employed to investigate the effect of nanoparticle agglomeration on the effective properties of the nanoparticle-filled polymer [39–41]. A number of nanoparticles are supposed to uniformly disperse into the polymer, and other nanoparticles appear in the agglomeration state. The whole volume of the nanoparticles in the RVE of the filled polymer specified by V_{NP} is divided into the following two parts:

$$V_{NP} = V_{NP}^{agg} + V_{NP}^{em} \tag{4}$$

where V_{NP}^{agg} is the volume of nanoparticles inside the agglomerated phase and V_{NP}^{em} denotes the volume of nanoparticles in the polymer matrix and outside the agglomerates. The definition of these two parameters for the agglomeration is as follows:

$$\zeta = \frac{V_{agg}}{V}, \quad \xi = \frac{V_{NP}^{agg}}{V_{NP}} \tag{5}$$

where V is the volume of the filled polymer RVE and V_{agg} denotes the volume of the agglomerate phase within the RVE [39–41]. Thus, the volume fraction of nanoparticles in the agglomeration phase ϕ_{NP}^{agg} and in the polymer matrix and outside the agglomerates ϕ_{NP}^{em} is determined as

$$\phi_{NP}^{agg} = \frac{V_{NP}^{agg}}{V_{agg}} = \frac{\zeta}{\xi} \phi_{NP}, \quad \phi_{NP}^{em} = \frac{V_{NP} - V_{NP}^{agg}}{V - V_{agg}} = \frac{1 - \zeta}{1 - \xi} \phi_{NP} \tag{6}$$

We analyze the nanoparticle-filled polymer as a system consisting of agglomerates of spherical shape embedded in a new matrix. We initially predict Young’s modulus and Poisson’s ratio of the agglomerate and the new matrix phases by the Ji model and the rule of mixture. The Young’s modulus and Poisson’s ratio are then used to calculate the bulk modulus and shear modulus. Using the bulk moduli and shear moduli of the agglomerate (K_{agg}, G_{agg}) and the new matrix (K_{em}, G_{em}), the equivalent bulk modulus (\bar{K}_{NC}) and shear modulus (\bar{G}_{NC}) of the nanoparticle-filled polymer system with the nanoparticle agglomeration are predicted by the Mori–Tanaka model [39–41], respectively,

$$\bar{K}_{NC} = K_{em} + \frac{\xi \left(\frac{K_{agg}}{K_{em}} - 1 \right)}{1 + \frac{1 - \xi}{1 + \frac{4G_{em}}{3K_{em}}} \left(\frac{K_{agg}}{K_{em}} - 1 \right)} K_{em}, \tag{7}$$

$$\bar{G}_{NC} = G_{em} + \frac{\xi \left(\frac{G_{agg}}{G_{em}} - 1 \right)}{1 + \frac{(6 + 12 \frac{G_{em}}{K_{em}})}{(15 + 20 \frac{G_{em}}{K_{em}})} (1 - \xi) \left(\frac{G_{agg}}{G_{em}} - 1 \right)} G_{em}. \tag{8}$$

Thus, the elastic properties of a nanoparticle-filled polymer considering the inter-phase region and agglomeration of nanoparticles can be achieved by the micromechanical technique developed in this section.

2.2. Piezoelectric Fiber Composites

Now, a micromechanical model can be adopted to estimate the equivalent properties of piezoelectric fibrous nanocomposites. By the means of the conventional indicial notation, the constitutive equations of piezoelectric materials are as follows [42–44]:

$$\begin{aligned} \sigma_{ij} &= C_{ijmn}\varepsilon_{mn} + e_{nij}E_n \\ D_i &= e_{imn}\varepsilon_{mn} - k_{in}E_n \end{aligned} \tag{9}$$

where the repeated sub-scripts are summed over the range of $i, j, m, n = 1, 2, 3$, and σ_{ij} and ε_{mn} stand for the stress and strain tensors, respectively. E_n and D_i stand for the electric field and the electric displacement vectors, respectively. C_{ijmn} , e_{nij} , and k_{in} denote the elastic stiffness and piezoelectric and permittivity tensors, respectively. Divergence equations expressing the mechanical equilibrium and Gauss' law can be given by Equation (10) [44], respectively:

$$\begin{aligned} \sigma_{ij,j} &= 0 \\ D_{i,i} &= 0 \end{aligned} \tag{10}$$

Moreover, the gradient equations defining the strain displacement equations and electric field potential are expressed, respectively:

$$\begin{aligned} \varepsilon_{ij} &= \frac{1}{2}(u_{i,j} + u_{j,i}) \\ E_i &= -\phi_{,i} \end{aligned} \tag{11}$$

in which u_i and ϕ stand for the mechanical displacement and electric potential, respectively.

The components of piezoelectric fibrous nanocomposites are the nanoparticle-filled polymer as the matrix phase and the piezoelectric fibers as the reinforcing phase. On the basis of the Mori–Tanaka micromechanical approach and considering v_m and v_r as the volume fraction of the matrix and fiber, respectively, the electro-elastic constants of piezoelectric fibrous nanocomposites can be estimated as

$$\tilde{\mathbf{C}}^c = \tilde{\mathbf{C}}^m + v_r \left(\tilde{\mathbf{C}}^r - \tilde{\mathbf{C}}^m \right) \mathbf{B} \tag{12}$$

in which $\tilde{\mathbf{C}}^r$ and $\tilde{\mathbf{C}}^m$ are the electro-elastic modulus matrices for the reinforcement and matrix, respectively, and the piezoelectric concentration tensor is defined as follows:

$$\mathbf{B} = \mathbf{A}[v_m\mathbf{I} + v_r\mathbf{A}]^{-1}, \mathbf{A} = \left[\mathbf{I} + \hat{\mathbf{S}} \left(\tilde{\mathbf{C}}^m \right)^{-1} \left(\tilde{\mathbf{C}}^r - \tilde{\mathbf{C}}^m \right) \right]^{-1}, \tag{13}$$

where $\hat{\mathbf{S}}$ is the Eshelby tensor and its components can be found in the literature [18,24,27,44]. It is worth mentioning that all simulation procedures and numerical results obtained in this research have been performed using codes written in MATLAB(R2024b) software. Also, it should be noted that all formulations used for the simulations in MATLAB software are analytical relations, and the finite element method has not been employed.

3. Results and Discussion

In this section, we first present the numerical results of the Young's moduli, shear moduli, and piezoelectric coefficients of PZT-7A fiber-reinforced nanocomposites with the silica-nanoparticle-filled polyimide matrix. Then, some comparisons are made between the present predictions and other results available in the literature [45,46].

3.1. Piezoelectro-Elastic Response of Piezoelectric Fibrous Nanocomposites

The micromechanical model consisting of Ji's model, the rule of mixture, and the Mori–Tanaka model is used to investigate the effective constants of the piezoelectric fibrous nanocomposite. The constituents of the composite are PZT-7A, polyimide, and silica nanoparticles. The

Young's modulus and Poisson's ratio of the polyimide and silica nanoparticles are 3.78 GPa and 0.4 and 73 GPa and 0.23 [20,22,44], respectively. Table 1 lists the properties of the PZT-7A fiber. The piezoelectric fiber volume fraction is considered to be 60%. The diameter of the silica nanoparticles and their volume fraction into the polyimide matrix are 30 nm and 3%, respectively. Also, the Young's modulus, Poisson's ratio, and thickness of the interphase region are taken as $E_i = 10E_m$, 0.4, and $t_i = 0.5d_{NP}$ [20,31], respectively.

Table 1. Material constants of PZT5 fiber, epoxy, and PZT-7A fiber [9,44].

Material	PZT5	Epoxy	PZT-7A
C_{11} (GPa)	121	8	148
C_{12} (GPa)	75.4	4.4	76.2
C_{13} (GPa)	75.2	4.4	74.2
C_{22} (GPa)	121	8	148
C_{23} (GPa)	75.2	4.4	74.2
C_{33} (GPa)	111	8	131
C_{44} (GPa)	21.1	1.8	25.4
C_{66} (GPa)	22.8	1.8	35.9
e_{31} (C/m ²)	−5.4	0	−2.1
e_{33} (C/m ²)	9.5	0	9.5

Figure 2 shows the influence of adding silica nanoparticles on the material constants of the piezoelectric fibrous nanocomposites. The numerical results are presented for two values of nanoparticle volume fraction (NPVF), 3% and 5%. The material properties of piezoelectric fibrous composites without nano-inclusions are also illustrated in the figure. Figure 2a indicates the results of the longitudinal Young's modulus versus piezoelectric fiber volume fraction. Incorporating nano-inclusions into the polymer matrix insignificantly affects the longitudinal Young's modulus. This is attributed to the fact that the longitudinal properties of long fiber-reinforced composites are mostly dominated by the material properties and content of fibers [9,18,47,48]. It can be seen in Figure 2a that Young's modulus in the direction parallel to the fiber direction linearly increases as the piezoelectric fiber volume fraction increases. Figure 2b shows the variation in the transverse Young's modulus of the piezoelectric fibrous nanocomposites with the piezoelectric fiber volume fraction. The transverse Young's modulus notably depends on the nanoparticles in the polyimide matrix. The value of E_T of the silica-nanoparticle-containing nanocomposite is greater than that of the composite without silica nanoparticles. When the piezoelectric fiber volume fraction is 60%, the nanocomposite with a 3% silica-nanoparticle-containing polyimide exhibits a 39% improvement in the transverse Young's modulus in comparison with the composite without nanoparticles. Adding silica nanoparticles within the polyimide provides a relatively stronger matrix that is potentially beneficial for the transverse Young's modulus of the piezoelectric fibrous nanocomposites. The increase in the silica nanoparticle amount aids the nanocomposite in obtaining a higher value of the transverse Young's modulus. A similar trend has been found for other types of nanofillers [9,18,48]. It is shown in Figure 2b that the Young's modulus in the direction perpendicular to the piezoelectric fiber nonlinearly increases as the fiber volume fraction increases. Based on the results observed in Figure 2c,d, adding silica nanoparticles is generally beneficial to shear moduli in the longitudinal and transverse directions. Both shear moduli are enhanced by increasing the piezoelectric fiber volume fraction. The values of the transverse shear modulus of the 60% piezoelectric-fiber-reinforced composite without nanoparticles and with a 3% nanoparticle content are calculated as 6.04 GPa and 7.96 GPa, respectively. Figure 2e depicts the piezoelectric coefficient e_{31} of the piezoelectric fibrous nanocomposites versus the piezoelectric fiber volume fraction. The value of piezoelectric coefficient e_{31} can be significantly improved as a result of the nanoparticle addition into the polyimide matrix. A major contribution to the piezoelectric coefficient e_{31} is from the polymer matrix properties. Compared to the piezoelectric fibrous composite, the piezoelectric coefficient e_{31} of the piezoelectric fibrous nanocomposite containing a 3% silica-nanoparticle-filled polyimide matrix exhibits an upward trend with an approximate 37% improvement. Therefore, in-

incorporating nanofillers into the polymer can enhance the in-plane actuation property of piezoelectric fibrous nanocomposites over that of a traditional piezoelectric fibrous composite without nanofillers. This trend has been reported for other composite systems containing CNTs [9,18,19]. The piezoelectric coefficient e_{31} of piezoelectric fibrous nanocomposites exhibits an improvement through the increase in the piezoelectric fiber volume fraction. Figure 2f displays the piezoelectric coefficient e_{33} versus the fiber volume fraction. There is no effect of silica nanoparticles on the piezoelectric coefficient e_{33} because its value is mostly dominated by the piezoelectric property of the fiber. A linear increase is obtained for the piezoelectric coefficient e_{33} as the piezoelectric fiber volume fraction increases. Because the piezoelectric constant e_{31} and the elastic properties such as E_T and G_{TL} of the piezoelectric fibrous nanocomposite containing silica nanoparticles are improved, this composite has good potential for use as a superior actuator material for intelligent structures with a great in-plane actuation option [9,12].

The micromechanical results for investigating the role of the interfacial zone between the silica nanoparticles and polyimide matrix in the material constants of the piezoelectric fibrous nanocomposites are presented in Figure 3. It is worth pointing out that the interphase does not have a notable contribution to the Young's modulus in the longitudinal direction, as seen in Figure 3a. It may be concluded from Figure 3b–d that the formation of the interfacial region is beneficial to the transverse Young's modulus and both shear moduli. Relative to the composite system without the interphase, an increasing trend is observed for these three elastic moduli of the nanocomposite with the interphase. The results of Figure 3e disclose that the interphase tends to improve the piezoelectric coefficient e_{31} . A literature survey shows that the interphase between the polymer matrix and CNTs can contribute to the improvement of the overall properties of piezoelectric–CNT nanocomposites [18]. As shown in Figure 3f, the piezoelectric coefficient e_{33} exhibits no variation in the presence or absence of the interphase.

Generally, the interphase has properties in between those of the nanoparticle and those of the polymer matrix [20,22,29,31,32,34]. To better evaluate the effect of interphase characteristics on the material constants of piezoelectric fibrous nanocomposites, a micromechanical analysis is conducted with different values of interphase stiffness and thickness. The results of the transverse Young's modulus, longitudinal shear modulus, transverse shear modulus, and piezoelectric coefficient e_{31} with changing the interphase elastic modulus are shown in Figure 4a–d, respectively. The effective properties of the piezoelectric fibrous nanocomposite can be enhanced with increasing the interphase elastic modulus. It is noted that a stiffer interphase can increase the mechanical properties of the polymer matrix [18,20,22,29]. One of the ways to enhance the mechanical properties of the interfacial region may be nanoparticle surface treatment.

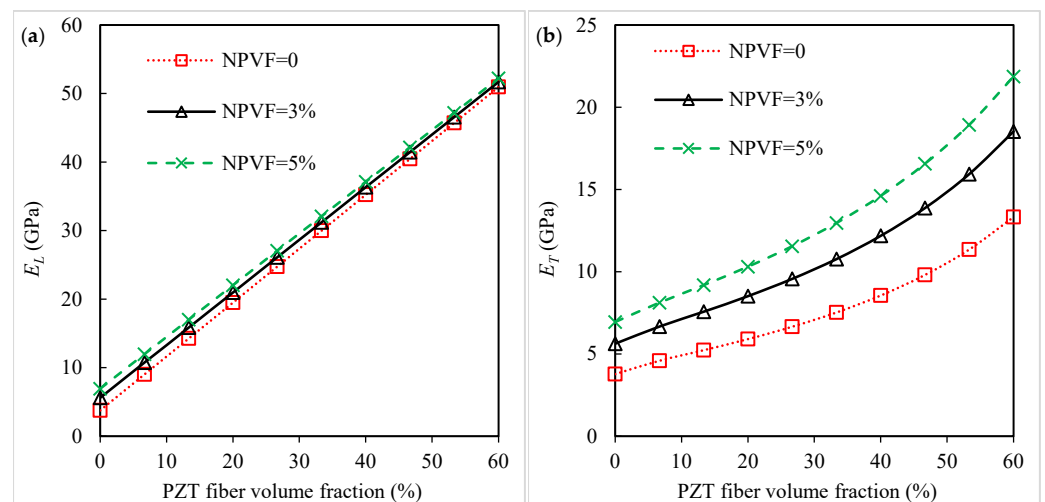


Figure 2. Cont.

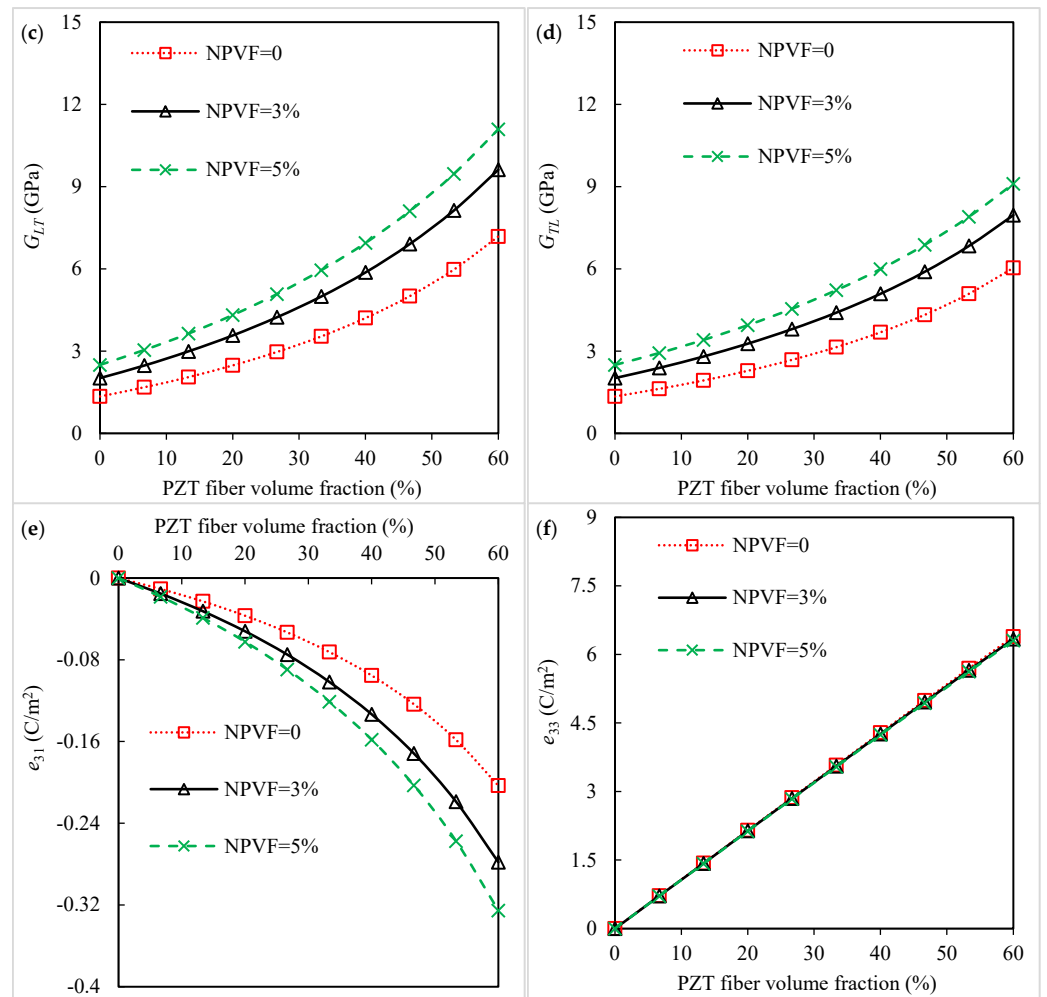


Figure 2. Influence of nanoparticle volume fraction on the (a) longitudinal Young's modulus, (b) transverse Young's modulus, (c) longitudinal shear modulus, (d) transverse shear modulus, (e) piezoelectric coefficient e_{31} , and (f) piezoelectric coefficient e_{33} of the piezoelectric fibrous nanocomposite containing silica nanoparticles.

The influence of changing the interphase thickness on the properties of nanocomposites, including E_T , G_{LT} , G_{TL} , and e_{31} , is depicted in Figure 5a–d, respectively. The increase in interphase thickness significantly improves the elastic and piezoelectric constants. Different methods for nanoparticle functionalization may produce interphases with variable thicknesses. By increasing the interphase thickness from 1 nm to 15 nm, the improvement in the transverse elastic modulus with a 3% silica-nanoparticle-containing polyimide matrix is calculated to be about 20.5%. In turn, for the piezoelectric coefficient e_{31} , the improvement is about 26%. It is worth mentioning that the in-plane actuation caused by the piezoelectric composite is increased by tailoring the piezoelectric constant e_{31} [9,47]. An important conclusion from the above micromechanical studies is the production of a stiff and thick interphase in the nanocomposite fabrication. This is due to the increased stiffness of the polymer matrix by adding nanoparticles, as reported in previous studies [18,20,22,29].

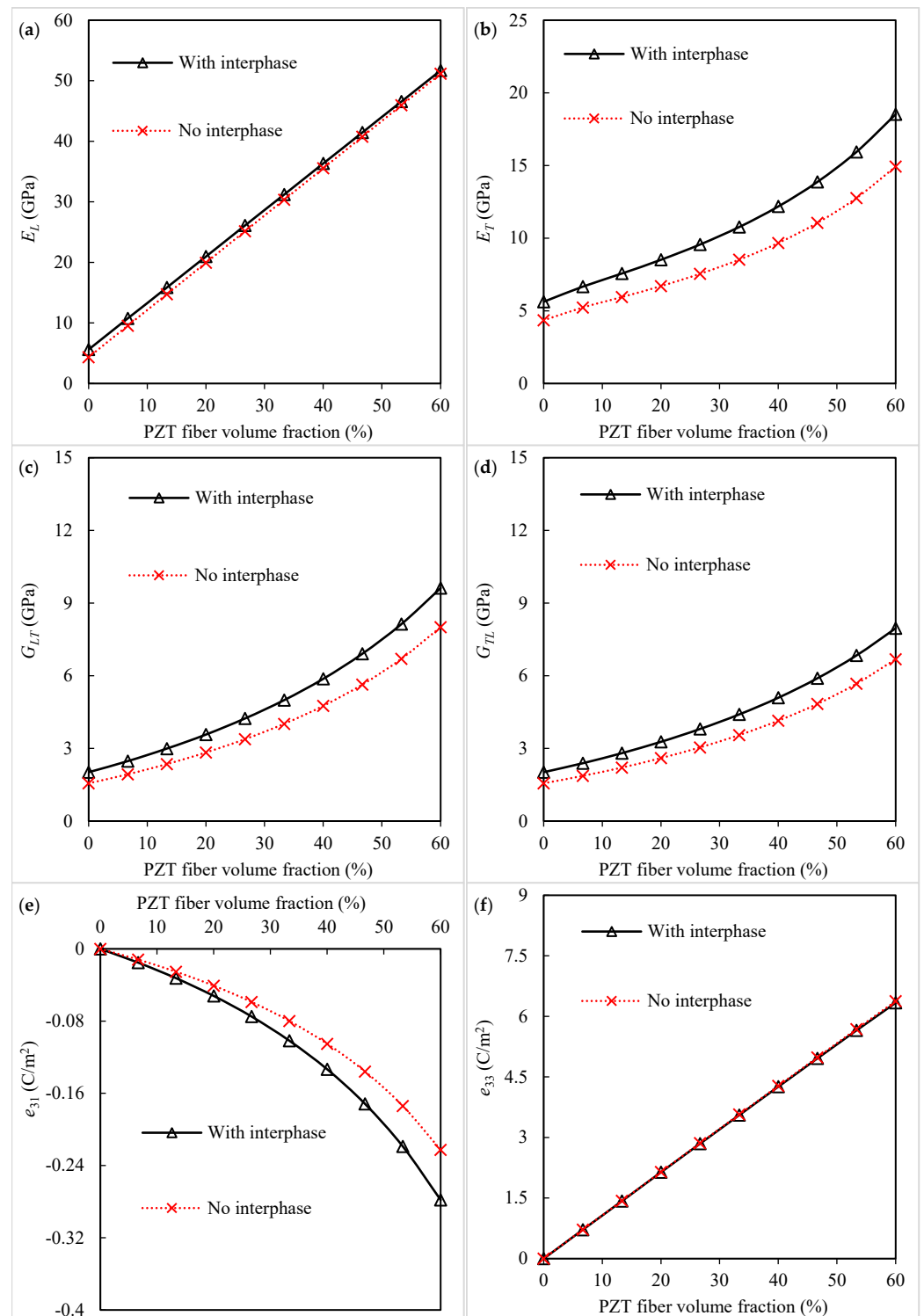


Figure 3. Influence of interphase region on the (a) longitudinal Young's modulus, (b) transverse Young's modulus, (c) longitudinal shear modulus, (d) transverse shear modulus, (e) piezoelectric coefficient e_{31} , and (f) piezoelectric coefficient e_{33} of the piezoelectric fibrous nanocomposite containing silica nanoparticles.

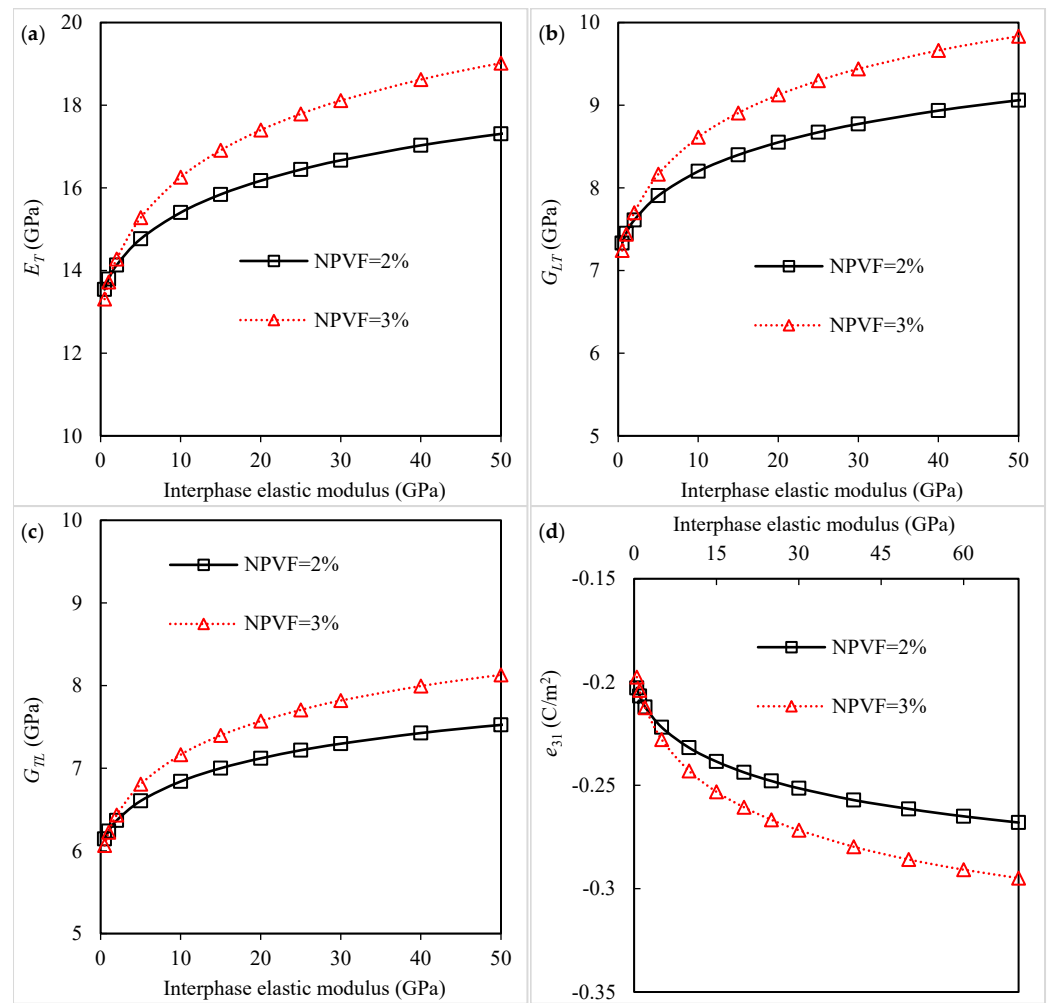


Figure 4. Variation in (a) transverse Young's modulus, (b) longitudinal shear modulus, (c) transverse shear modulus, and (d) piezoelectric coefficient e_{31} of piezoelectric fibrous nanocomposite with interphase elastic modulus.

The influence of the silica nanoparticle diameter on the mechanical properties and piezoelectric coefficients of piezoelectric fibrous nanocomposites is studied, and the results are displayed in Figure 6. As seen in Figure 6a, the values for the longitudinal Young's modulus with different nanoparticle diameters are close to each other, indicating the insignificant contribution of nanoparticle size to this elastic property. It is seen from Figure 6b that the addition of uniformly dispersed silica nanoparticles with smaller sizes results in an increase in the Young's modulus in the transverse direction. This may be explained by the interphase contribution to the final properties of nanocomposites becoming more prominent as the nanoparticle size decreases [20,48]. A notable enhancement in the shear moduli along both the longitudinal and transverse directions can be observed by the decrease in nanoparticle size, as shown in Figure 6c,d. The results of Figure 6e disclose that a smaller size of silica nanoparticles is required so as to further improve the piezoelectric coefficient e_{31} of the nanocomposites. In the case of the nanocomposite with a 3% silica-nanoparticle-containing polyimide matrix, the improvement is about 50% by decreasing the nanoparticle diameter from 100 nm to 20 nm. As $d_{NP} > 100$ nm, the change in nanoparticle diameter does not affect the elastic moduli or the piezoelectric coefficient e_{31} . The main reason for this behavior may be the reduced effect of the interphase. As the size of the nanoscale particles increases and goes to the microscale, the role of the interphase in the effective properties of the nanocomposites decreases. According to the outcomes of Figure 6f, the piezoelectric coefficient e_{33} of the nanocomposites does not depend on the nano-inclusion size since

the piezoelectric fibers have the main role in this property. Thus, the hybridization of the piezoelectric fibers with smaller nanoparticles induces better elastic moduli E_T , G_{LT} , and G_{TL} and a better piezoelectric coefficient e_{31} .

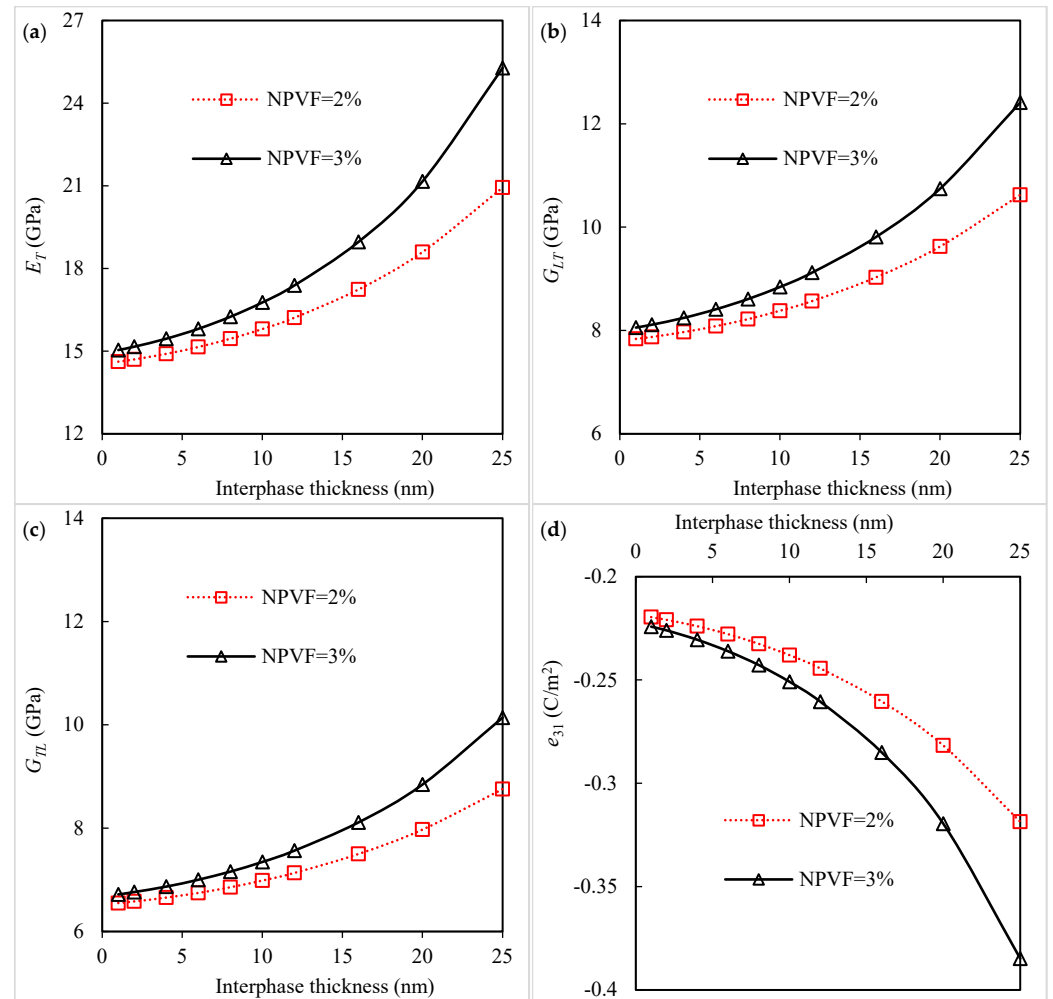


Figure 5. Variation in (a) transverse Young’s modulus, (b) longitudinal shear modulus, (c) transverse shear modulus, and (d) piezoelectric coefficient e_{31} of piezoelectric fibrous nanocomposite with interphase thickness.

To study the effect of dispersion quality of silica nanoparticles, the elastic moduli and piezoelectric coefficients of the piezoelectric fibrous nanocomposites are calculated for two conditions, including a uniform dispersion and an agglomerated state ($\zeta = 0.9$, $\xi = 0.1$). The numerical results of the micromechanical analysis are presented in Figure 7a–f. In this sensitivity study, the nanoparticle volume fraction is 5%. It is observed from Figure 7a that the longitudinal Young’s modulus is minimally affected by the non-uniform dispersion of the nanoparticles. The other three elastic constants, the transverse Young’s modulus, longitudinal shear modulus, and transverse shear modulus, appear to significantly decrease due to the formation of silica nanoparticle agglomeration (Figure 7b–d). The agglomeration of the silica nanoparticles produces a negative effect on the piezoelectric coefficient e_{31} . As compared to the uniformly dispersed case, a decrease of about 29.2% in the piezoelectric coefficient e_{31} is observed by forming the agglomeration. As mentioned in previous studies [20,37,38,48], nanoparticle agglomeration leads to a reduction in the mechanical properties of polymer matrix nanocomposites. The nanocomposite containing uniformly dispersed silica nanoparticles exhibits a higher piezoelectric coefficient e_{31} than that containing agglomerated nanoparticles. It is shown in Figure 7f that the dispersion quality does not affect the estimated piezoelectric

coefficient e_{33} . Uniformly dispersing and avoiding the agglomeration of nanoparticles into the polymer matrix are critical for advanced composite materials to take the maximum material constants, i.e., E_T , G_{LT} , G_{TL} , and e_{31} .

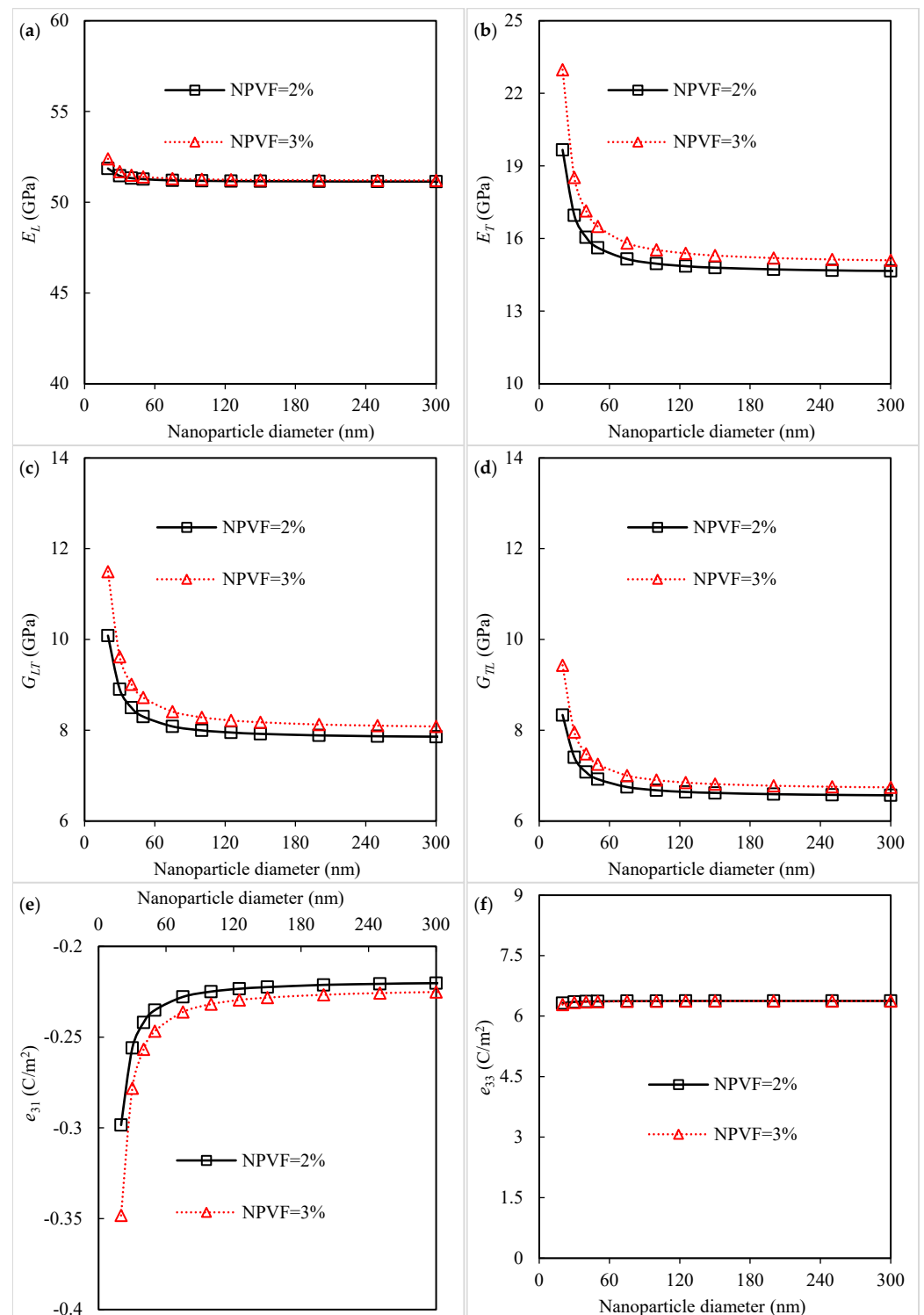


Figure 6. Influence of silica nanoparticle diameter on the (a) longitudinal Young's modulus, (b) transverse Young's modulus, (c) longitudinal shear modulus, (d) transverse shear modulus, (e) piezoelectric coefficient e_{31} , and (f) piezoelectric coefficient e_{33} of the piezoelectric fibrous nanocomposite containing silica nanoparticles.

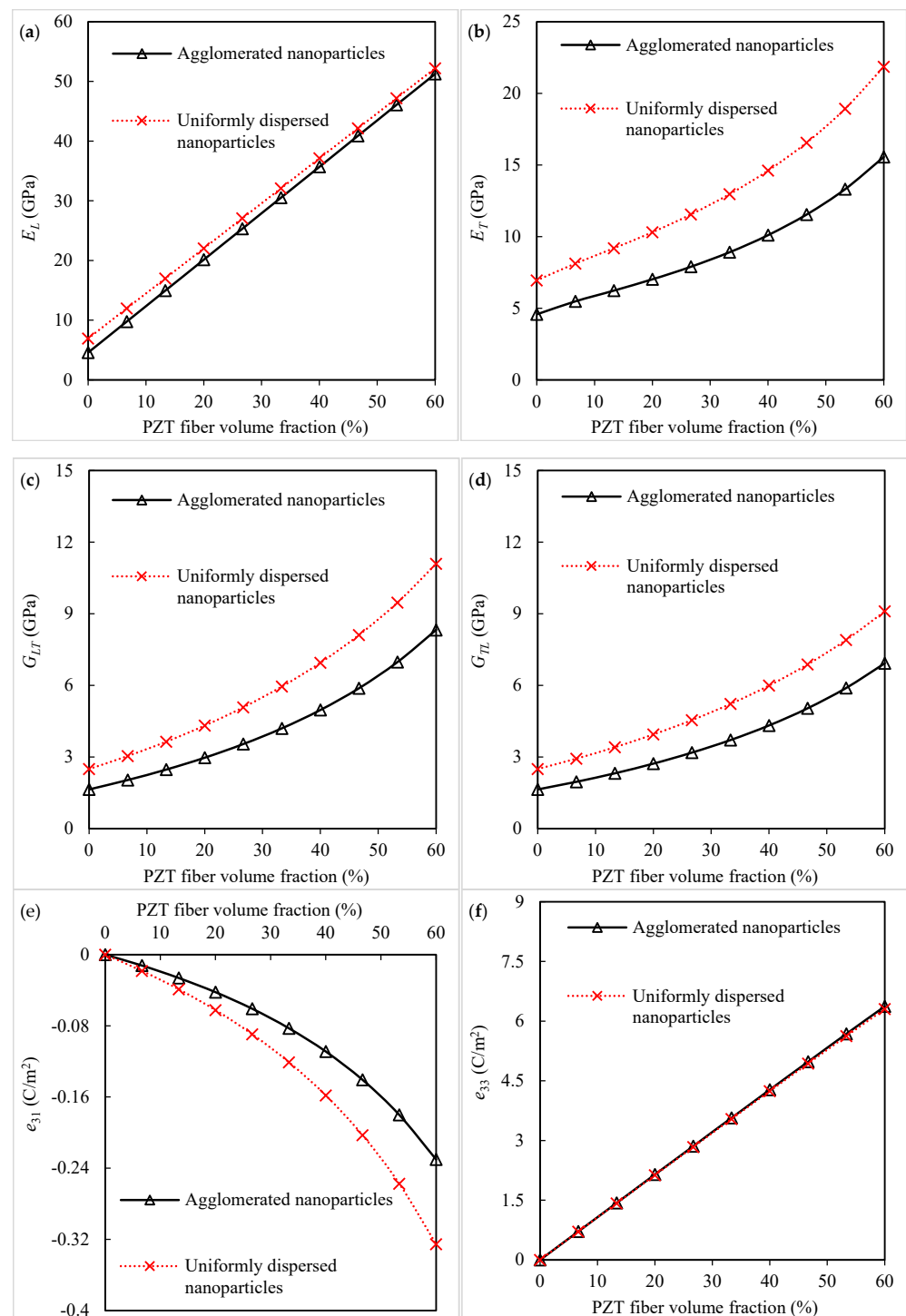


Figure 7. Influence of silica nanoparticle dispersion quality on the (a) longitudinal Young's modulus, (b) transverse Young's modulus, (c) longitudinal shear modulus, (d) transverse shear modulus, (e) piezoelectric coefficient e_{31} , and (f) piezoelectric coefficient e_{33} of the piezoelectric fibrous nanocomposite containing silica nanoparticles.

The results of the micromechanical analysis with silica and alumina nanoparticles individually incorporated into the polyimide matrix are presented in Figure 8. The volume fraction and diameter for both nanoparticles are identical. The influence of the interphase stiffness on the effective properties of the piezoelectric fibrous nanocomposites is also examined. The change in the interphase stiffness is taken in a range from the soft material

to the stiff material. The soft interphase ($E_{i,soft}$) can be categorized as the material having very low stiffness in comparison with the reinforcement stiffness [49] as

$$E_{i,soft} = \frac{E_{NP} + E_m}{20} \quad (14)$$

The stiff interphase ($E_{i,stiff}$) can be categorized as the material having an average value of reinforcement and matrix stiffness and is very high in comparison with the matrix stiffness [49] as

$$E_{i,stiff} = \frac{E_{NP} + E_m}{2} \quad (15)$$

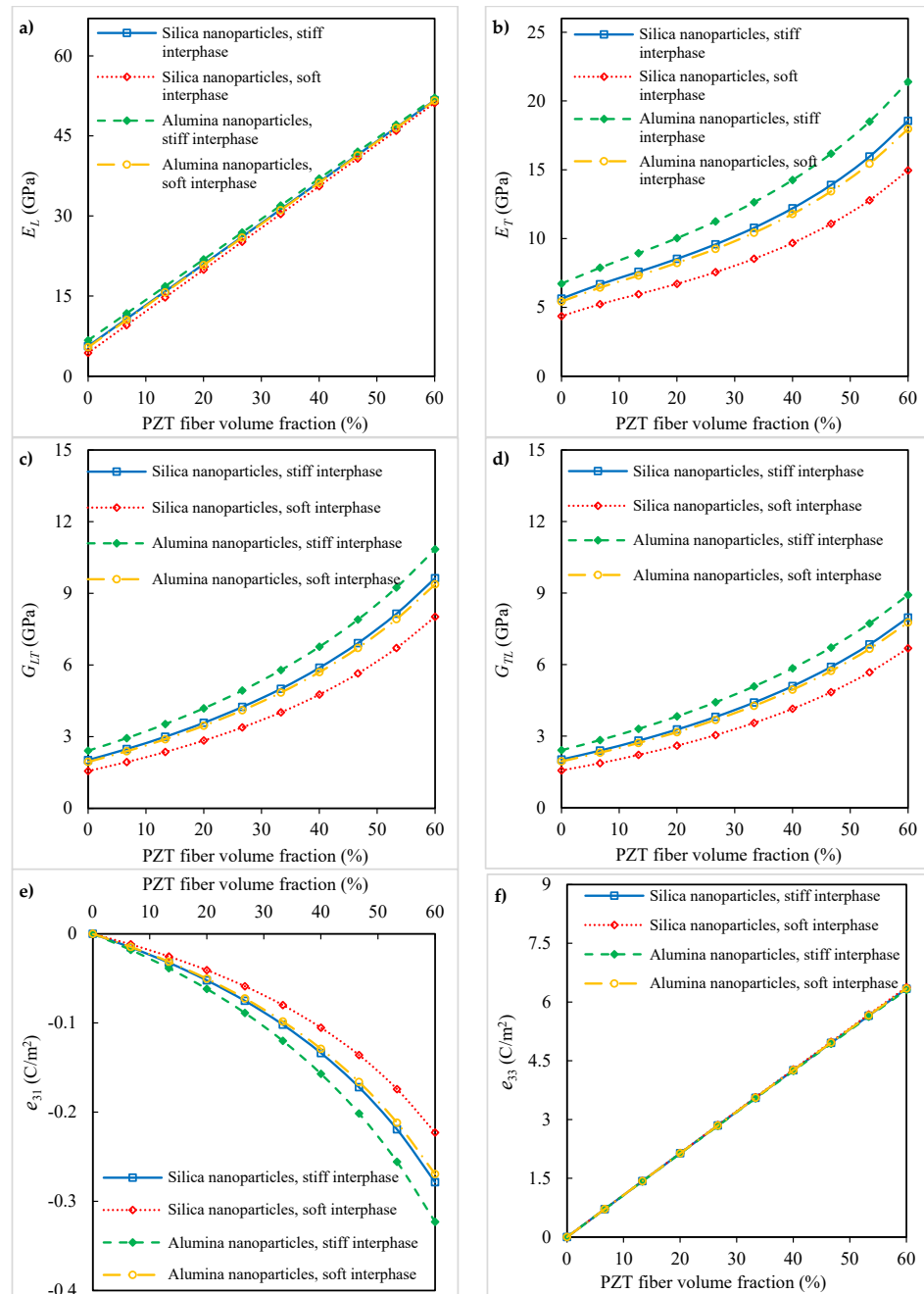


Figure 8. Influence of nanoparticle types on the (a) longitudinal Young’s modulus, (b) transverse Young’s modulus, (c) longitudinal shear modulus, (d) transverse shear modulus, (e) piezoelectric coefficient e_{31} , and (f) piezoelectric coefficient e_{33} of the piezoelectric fibrous nanocomposite containing nanoparticles.

On the basis of the outcomes shown in Figure 8a,f, the incorporation of different types of nano-inclusions has a negligible effect on the longitudinal Young's modulus and piezoelectric coefficient e_{33} . In contrast, changes in the nano-inclusion type embedded within the matrix affect the elastic moduli E_T , G_{LT} , and G_{TL} and the piezoelectric coefficient e_{31} of the nanocomposites, as shown in Figure 8b–e. Compared to the silica nanoparticles, the use of alumina nanoparticles in the polyimide matrix can further improve these material properties. Again, nanocomposites with a stiff interphase show higher elastic moduli E_T , G_{LT} , and G_{TL} and a higher piezoelectric coefficient e_{31} than those with a soft interphase. Due to the good mechanical and piezoelectric properties, the piezoelectric fiber–nanoparticle–polymer nanocomposites can find various industrial applications, such as in actuators, sensors, and energy-harvesting devices [9,12,26].

3.2. Comparisons with Experimental and Numerical Results

Now, the predictions are compared with the available experimental data of some silica-filled polymer composites for validating the micromechanical model. Figure 9 presents a comparison between the present predictions and experimental data [45] of the Young's modulus of silica-nanoparticle-filled poly(ether-ether-ketone) (PEEK) nanocomposites. Micromechanical tests are carried out in two different states: (1) in the presence of an interphase with $k = 5$, $t_i = 0.25 \times d_{NP}$ and (2) in the absence of an interphase. The silica nanoparticles with a mean diameter ~ 30 nm are uniformly dispersed in the polymer matrix. The Young's moduli of the silica nanoparticle and PEEK matrix are 73 GPa and 3.9 GPa, respectively. Figure 9 shows that the model without the interphase agrees better with the experiments for lower values of nanoparticle volume fraction. However, at higher nanoparticle contents, the model predictions with the interfacial region between the nanoparticles and polymer matrix give a more reasonable agreement as compared to the experiments [45]. The interphase region with a higher Young's modulus than that of the matrix material increases the Young's modulus of the nanocomposites significantly.

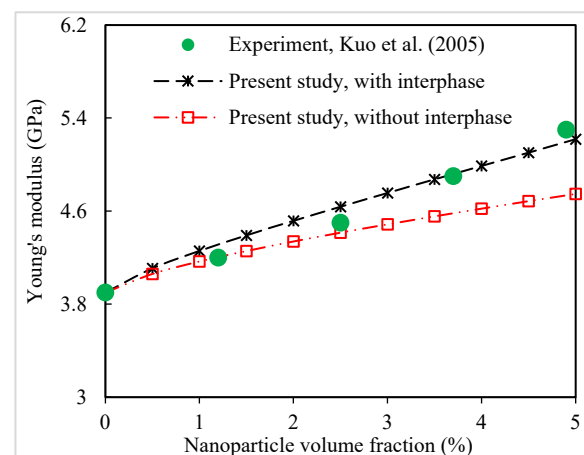


Figure 9. Present predictions for Young's modulus of silica-nanoparticle-filled PEEK nanocomposites compared to experimental data [45].

The Young's modulus of the silica-nanoparticle-filled nylon-6 nanocomposites determined by the present micromechanics method are compared with the experimental data [46]. Figure 10 shows the outcome of this comparison. The effect of considering the interphase in the micromechanical modeling on the final elastic modulus is also examined. It is observed that the two sets of results evaluated by the micromechanical model by taking the interphase region and the experimental route are in a good agreement.

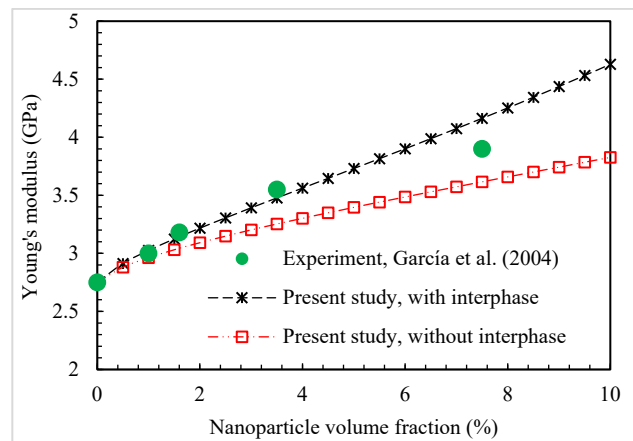


Figure 10. Present predictions for Young’s modulus of silica-nanoparticle-filled nylon-6 nanocomposites compared to experimental data [46].

In another comparison, two effective properties of the PZT5-fiber-reinforced epoxy composite including the elastic constant C_{33} and piezoelectric coefficient e_{31} predicted by the present micromechanical model are compared with the Mori–Tanaka predictions carried out in [9]. The material constants of the PZT5 fiber as well as the epoxy are given in Table 1 [9,44]. It is shown in Figure 11a,b that the two sets of results are in a very good agreement for both effective constants.

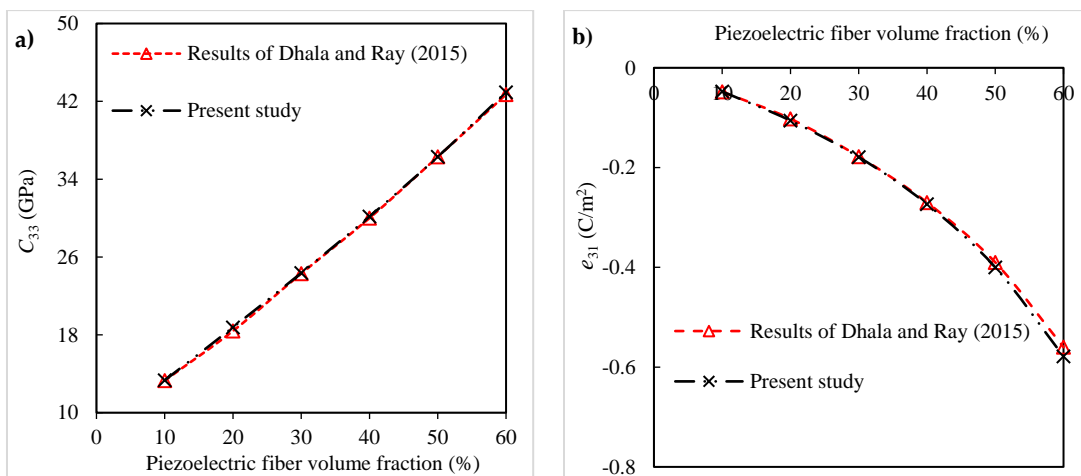


Figure 11. Comparison between the results of the present model and results of [9] for (a) elastic constant C_{33} and (b) piezoelectric coefficient e_{31} of PZT5-fiber-reinforced epoxy composites.

Wang et al. [50] used silica nanoparticles to produce a polymer nanocomposite: methyl methacrylate (MMA) was chosen as the matrix and copolymerized with a low amount of cationic functional comonomer 2-(methacryloyloxy)ethyltrimethylammonium chloride (MTC). Figure 12 shows another comparison between the present predictions and experimental measurements [50] for the Young’s modulus of silica-nanoparticle-filled P(MMA-co-MTC) nanocomposites. Silica nanoparticles have an average diameter of around 20 nm [50]. A good agreement is observed between the model predictions and the experimental measurements at all nanoparticle contents.

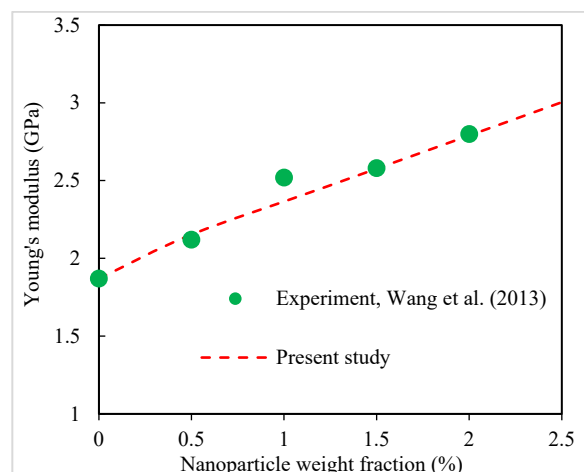


Figure 12. Present predictions for Young's modulus of silica-nanoparticle-filled P(MMA-co-MTC) nanocomposites compared to experimental data [50].

4. Conclusions

In this paper, the piezoelectro-elastic coefficients of PZT-7A-fiber-reinforced nanocomposites with a silica-nanoparticle-filled polyimide matrix were evaluated. First, the Ji and Mori–Tanaka models were hierarchically employed to predict the elastic properties of the silica-nanoparticle-filled polymer. The nanoparticle–polymer interphase and the nanoparticle agglomeration were included in the analysis. Then, considering the nanoparticle-filled polymer as the matrix and the piezoelectric fiber as the reinforcement, the Mori–Tanaka model was employed to predict the elastic and piezoelectric constants of the piezoelectric fibrous nanocomposites. A good agreement was observed between the present predictions and other results available in the literature. The results showed that adding silica nanoparticles into the polyimide matrix improves the elastic and piezoelectric properties (E_T , G_{LT} , G_{TL} , and e_{31}) of the piezoelectric fibrous nanocomposites. As compared to the composite without nanoparticles, 39%, 31.8%, and 37% improvements in the values of E_T , G_{TL} , and the piezoelectric coefficient e_{31} were observed once the volume fractions of the fiber and nanoparticle were 60% and 3%, respectively. More improvement in the elastic moduli E_T , G_{LT} , and G_{TL} and the piezoelectric coefficient e_{31} was found by decreasing the nanoparticle diameter. A thicker and stiffer interphase led to an increase in the elastic moduli E_T , G_{LT} , and G_{TL} and the piezoelectric coefficient e_{31} of the piezoelectric fibrous nanocomposites. However, the nanoparticle agglomeration that formed in the polymer matrix decreased the elastic moduli E_T , G_{LT} , and G_{TL} and the piezoelectric coefficient e_{31} . It was observed that increasing the piezoelectric fiber volume fraction increased the piezoelectro-elastic constants of the piezoelectric fibrous nanocomposites.

Author Contributions: Conceptualization, U.U.; methodology, U.U.; software, U.U., S.H.M. and M.K.A.; validation, U.U.; formal analysis, M.H.A.; investigation, S.H.M.; resources, S.H.M. and F.A.; writing—original draft, U.U.; writing—review and editing, S.H.M. and M.K.A.; visualization, M.H.A.; supervision, F.A. and M.K.A.; project administration, M.H.A., F.A. and M.K.A.; funding acquisition, F.A. All authors have read and agreed to the published version of the manuscript.

Funding: This research was funded through the Research Institute Supporting Program (RICSP-24-2), King Saud University, Riyadh, Saudi Arabia.

Institutional Review Board Statement: Not applicable.

Data Availability Statement: The original contributions presented in the study are included in the article, further inquiries can be directed to the corresponding author.

Acknowledgments: The authors extend their appreciation to the King Saud University for funding this work through the Research Institute Supporting Program (RICSP-24-2), King Saud University, Riyadh, Saudi Arabia.

Conflicts of Interest: The authors declare no conflict of interest.

References

1. Xu, L.F.; Yu, T.C.; Feng, X.; Yang, C.P.; Chen, Y.; Chen, W.; Zhou, J. Dimension dependence of thickness resonance behavior of piezoelectric fiber composites. *Mater. Chem. Phys.* **2018**, *218*, 34–38. [[CrossRef](#)]
2. Tan, D.; Yavarow, P.; Erturk, A. Nonlinear elastodynamics of piezoelectric macro-fiber composites with interdigitated electrodes for resonant actuation. *Compos. Struct.* **2018**, *187*, 137–143. [[CrossRef](#)]
3. Zhou, B.; Ma, X.; Xue, S. Nonlinear analysis of laminated beams with braided fiber piezoelectric composite actuators. *Int. J. Appl. Mech.* **2020**, *12*, 2050043. [[CrossRef](#)]
4. Su, Y.; Li, W.; Yuan, L.; Chen, C.; Pan, H.; Xie, G.; Conta, G.; Ferrier, S.; Zhao, X.; Chen, G.; et al. Piezoelectric fiber composites with polydopamine interfacial layer for self-powered wearable biomonitoring. *Nano Energy* **2021**, *89*, 106321. [[CrossRef](#)]
5. He, Z.; Liu, J.; Chen, Q. Higher-order asymptotic homogenization for piezoelectric composites. *Int. J. Solids Struct.* **2023**, *264*, 112092. [[CrossRef](#)]
6. Yu, Y.; Narita, F. Evaluation of electromechanical properties and conversion efficiency of piezoelectric nanocomposites with carbon-fiber-reinforced polymer electrodes for stress sensing and energy harvesting. *Polymers* **2021**, *13*, 3184. [[CrossRef](#)]
7. Tang, T.; Yu, W. Variational asymptotic micromechanics modeling of heterogeneous piezoelectric materials. *Mech. Mater.* **2008**, *40*, 812–824. [[CrossRef](#)]
8. Keramati, Y.; Ansari, R.; Hassanzadeh-Aghdam, M.K. Effect of graphene nano-sheets on the elastic and piezoelectric coefficients of unidirectional PZT-7A/polyimide hybrid composites. *J. Intell. Mater. Syst. Struct.* **2023**, *34*, 1548–1560. [[CrossRef](#)]
9. Dhala, S.; Ray, M.C. Micromechanics of piezoelectric fuzzy fiber-reinforced composite. *Mech. Mater.* **2015**, *81*, 1–17. [[CrossRef](#)]
10. Al Mahmud, H.; Radue, M.S.; Chinkanjanarot, S.; Pisani, W.A.; Gowtham, S.; Odegard, G.M. Multiscale modeling of carbon fiber-graphene nanoplatelet-epoxy hybrid composites using a reactive force field. *Compos. Part B Eng.* **2019**, *172*, 628–635. [[CrossRef](#)]
11. Sahu, R.; Ponnusami, S.A.; Weimer, C.; Harursampath, D. Interface engineering of carbon fiber composites using CNT: A review. *Polym. Compos.* **2024**, *45*, 9–42. [[CrossRef](#)]
12. Keramati, Y.; Ansari, R.; Hassanzadeh-Aghdam, M.K.; Umer, U. Micromechanical simulation of thermal expansion, elastic stiffness and piezoelectric constants of graphene/unidirectional BaTiO₃ fiber reinforced epoxy hybrid nanocomposites. *Acta Mech.* **2023**, *234*, 6251–6270. [[CrossRef](#)]
13. Cui, X.; Liu, J.; Liu, H.; Wu, G. Enhanced interfacial strength and mechanical properties of carbon fiber composites by introducing functionalized silica nanoparticles into the interface. *J. Adhes. Sci. Technol.* **2019**, *33*, 479–492. [[CrossRef](#)]
14. Hwayyin, R.N.; Hussien, S.K.; Ameen, A.S. The effect of nano-silica on the mechanical properties of composite polyester/carbon fibers. *J. Mech. Eng. Sci.* **2022**, *16*, 9175–9186. [[CrossRef](#)]
15. Zheng, Y.; Ning, R.; Zheng, Y. Study of SiO₂ nanoparticles on the improved performance of epoxy and fiber composites. *J. Reinf. Plast. Compos.* **2005**, *24*, 223–233. [[CrossRef](#)]
16. Gang, D.; Chilan, C.; Haobin, T.; Zhenhua, L.; Dingzhong, Z.; Kang, Q. The research on the effect of SiO₂ and CF on the tensile and tribological properties of PI composite. *Proc. Inst. Mech. Eng. Part J J. Eng. Tribol.* **2015**, *229*, 1513–1518. [[CrossRef](#)]
17. Tang, Y.; Ye, L.; Zhang, D.; Deng, S. Characterization of transverse tensile, interlaminar shear and interlaminar fracture in CF/EP laminates with 10 wt% and 20 wt% silica nanoparticles in matrix resins. *Compos. Part A Appl. Sci. Manuf.* **2011**, *42*, 1943–1950. [[CrossRef](#)]
18. Hasanzadeh, M.; Ansari, R.; Hassanzadeh-Aghdam, M.K. Evaluation of effective properties of piezoelectric hybrid composites containing carbon nanotubes. *Mech. Mater.* **2019**, *129*, 63–79. [[CrossRef](#)]
19. Godara, S.S.; Mahato, P.K. Micromechanical technique based prediction of effective properties for hybrid smart nanocomposites. *Mech. Adv. Mater. Struct.* **2022**, *29*, 2065–2073. [[CrossRef](#)]
20. Boutaleb, S.; Zaïri, F.; Mesbah, A.; Nait-Abdelaziz, M.; Gloaguen, J.M.; Boukharouba, T.; Lefebvre, J.M. Micromechanics-based modelling of stiffness and yield stress for silica/polymer nanocomposites. *Int. J. Solids Struct.* **2009**, *46*, 1716–1726. [[CrossRef](#)]
21. Kontou, E.; Christopoulos, A.; Koralli, P.; Mouzakis, D.E. The effect of silica particle size on the mechanical enhancement of polymer nanocomposites. *Nanomaterials* **2023**, *13*, 1095. [[CrossRef](#)]
22. Sun, L.; Gibson, R.F.; Gordaninejad, F. Multiscale analysis of stiffness and fracture of nanoparticle-reinforced composites using micromechanics and global–local finite element models. *Eng. Fract. Mech.* **2011**, *78*, 2645–2662. [[CrossRef](#)]
23. Ray, M.C. Micromechanics of piezoelectric composites with improved effective piezoelectric constant. *Int. J. Mech. Mater. Des.* **2006**, *3*, 361–371. [[CrossRef](#)]
24. Dinartz, F.; Sabar, H. Magneto-electro-elastic coated inclusion problem and its application to magnetic-piezoelectric composite materials. *Int. J. Solids Struct.* **2011**, *48*, 2393–2401. [[CrossRef](#)]
25. Koutsawa, Y. Overall thermo-magneto-electro-elastic properties of multiferroics composite materials with arbitrary heterogeneities spatial distributions. *Compos. Struct.* **2015**, *133*, 764–773. [[CrossRef](#)]
26. Ferreira, P.M.; Machado, M.A.; Vidal, C.; Carvalho, M.S. Modelling electro-mechanical behaviour in piezoelectric composites: Current status and perspectives on homogenisation. *Adv. Eng. Softw.* **2024**, *193*, 103651. [[CrossRef](#)]
27. Mishra, N.; Das, K. A Mori–Tanaka based micromechanical model for predicting the effective electroelastic properties of orthotropic piezoelectric composites with spherical inclusions. *SN Appl. Sci.* **2020**, *2*, 1206. [[CrossRef](#)]

28. Pan, J.; Bian, L. A physics investigation for influence of carbon nanotube agglomeration on thermal properties of composites. *Mater. Chem. Phys.* **2019**, *236*, 121777. [[CrossRef](#)]
29. Mortazavi, B.; Bardoun, J.; Ahzi, S. Interphase effect on the elastic and thermal conductivity response of polymer nanocomposite materials: 3D finite element study. *Comput. Mater. Sci.* **2013**, *69*, 100–106. [[CrossRef](#)]
30. Ghasemi, A.R.; Hosseinpour, K. The SWCNTs roles in stress/strain distribution of three-phase multilayered nanocomposite cylinder under combined internal pressure and thermo-mechanical loading. *J. Braz. Soc. Mech. Sci. Eng.* **2018**, *40*, 391. [[CrossRef](#)]
31. Cannillo, V.; Bondioli, F.; Lusvarghi, L.; Montorsi, M.; Avella, M.; Errico, M.E.; Malinconico, M. Modeling of ceramic particles filled polymer–matrix nanocomposites. *Compos. Sci. Technol.* **2006**, *66*, 1030–1037. [[CrossRef](#)]
32. Snipes, J.S.; Robinson, C.T.; Baxter, S.C. Effects of scale and interface on the three-dimensional micromechanics of polymer nanocomposites. *J. Compos. Mater.* **2011**, *45*, 2537–2546. [[CrossRef](#)]
33. Nematollahi, H.; Mohammadi, M.; Munir, M.T.; Zare, Y.; Rhee, K.Y. Two-Step Method for Predicting Young’s Modulus of Nanocomposites Containing Nanodiamond Particles. *J. Mater. Res. Technol.* **2024**, *33*, 2343–2352. [[CrossRef](#)]
34. Pakseresht, M.; Ansari, R.; Hassanzadeh-Aghdam, M.K. An efficient homogenization scheme for analyzing the elastic properties of hybrid nanocomposites filled with multiscale particles. *J. Braz. Soc. Mech. Sci. Eng.* **2021**, *43*, 3. [[CrossRef](#)]
35. Ji, X.L.; Jing, J.K.; Jiang, W.; Jiang, B.Z. Tensile modulus of polymer nanocomposites. *Polym. Eng. Sci.* **2002**, *42*, 983–993. [[CrossRef](#)]
36. Zare, Y. Assumption of interphase properties in classical Christensen–Lo model for Young’s modulus of polymer nanocomposites reinforced with spherical nanoparticles. *RSC Adv.* **2015**, *5*, 95532–95538. [[CrossRef](#)]
37. Zhang, H.; Zhang, Z.; Friedrich, K.; Eger, C. Property improvements of in situ epoxy nanocomposites with reduced interparticle distance at high nanosilica content. *Acta Mater.* **2006**, *54*, 1833–1842. [[CrossRef](#)]
38. Naito, K. Tensile properties of polyacrylonitrile-and pitch-based hybrid carbon fiber/polyimide composites with some nanoparticles in the matrix. *J. Mater. Sci.* **2013**, *48*, 4163–4176. [[CrossRef](#)]
39. Ji, X.Y.; Cao, Y.P.; Feng, X.Q. Micromechanics prediction of the effective elastic moduli of graphene sheet-reinforced polymer nanocomposites. *Model. Simul. Mater. Sci. Eng.* **2010**, *18*, 045005. [[CrossRef](#)]
40. Dastgerdi, J.N.; Marquis, G.; Salimi, M. The effect of nanotubes waviness on mechanical properties of CNT/SMP composites. *Compos. Sci. Technol.* **2013**, *86*, 164–169. [[CrossRef](#)]
41. Shi, D.L.; Feng, X.Q.; Huang, Y.Y.; Hwang, K.C.; Gao, H. The effect of nanotube waviness and agglomeration on the elastic property of carbon nanotube-reinforced composites. *J. Eng. Mater. Technol.* **2004**, *126*, 250–257. [[CrossRef](#)]
42. Mallik, N.; Ray, M.C. Effective coefficients of piezoelectric fiber-reinforced composites. *AIAA J.* **2003**, *41*, 704–710. [[CrossRef](#)]
43. Aboudi, J.; Arnold, S.M.; Bednarczyk, B.A. *Micromechanics of Composite Materials: A Generalized Multiscale Analysis Approach*; Butterworth-Heinemann: Oxford, UK, 2013.
44. Odegard, G.M. Constitutive modeling of piezoelectric polymer composites. *Acta Mater.* **2004**, *52*, 5315–5330. [[CrossRef](#)]
45. Kuo, M.C.; Tsai, C.M.; Huang, J.C.; Chen, M. PEEK composites reinforced by nano-sized SiO₂ and Al₂O₃ particulates. *Mater. Chem. Phys.* **2005**, *90*, 185–195. [[CrossRef](#)]
46. García, M.; van Vliet, G.; ten Cate, M.G.; Chavez, F.; Norder, B.; Kooi, B.; van Zyl, W.E.; Verweij, H.; Blank, D.H.A. Large-scale extrusion processing and characterization of hybrid nylon-6/SiO₂ nanocomposites. *Polym. Adv. Technol.* **2004**, *15*, 164–172. [[CrossRef](#)]
47. Ray, M.C. The concept of a novel hybrid smart composite reinforced with radially aligned zigzag carbon nanotubes on piezoelectric fibers. *Smart Mater. Struct.* **2010**, *19*, 035008. [[CrossRef](#)]
48. Mahmoodi, M.J.; Hassanzadeh-Aghdam, M.K.; Safi, M. Effects of nano-sized silica particles on the off-axis creep performance of unidirectional fiber-reinforced polymer hybrid composites. *J. Compos. Mater.* **2021**, *55*, 1575–1589. [[CrossRef](#)]
49. Joshi, P.; Upadhyay, S.H. Effect of interphase on elastic behavior of multiwalled carbon nanotube reinforced composite. *Comput. Mater. Sci.* **2014**, *87*, 267–273. [[CrossRef](#)]
50. Wang, X.; Wang, L.; Su, Q.; Zheng, J. Use of unmodified SiO₂ as nanofiller to improve mechanical properties of polymer-based nanocomposites. *Compos. Sci. Technol.* **2013**, *89*, 52–60. [[CrossRef](#)]

Disclaimer/Publisher’s Note: The statements, opinions and data contained in all publications are solely those of the individual author(s) and contributor(s) and not of MDPI and/or the editor(s). MDPI and/or the editor(s) disclaim responsibility for any injury to people or property resulting from any ideas, methods, instructions or products referred to in the content.